Paper 117

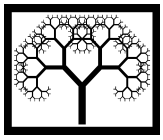

Proceedings of the Eighth International Conference on Engineering Computational Technology, B.H.V. Topping, (Editor), Civil-Comp Press, Stirlingshire, Scotland

Multi-Physics Computational Fluid Dynamics Modelling of Three-Phase Flow in a Nano-Particle Separator using the Particle-Based Method

R. Takahashi[1], M. Suzuki[2], M. Yamamoto[2] and H. Kitada[3]
[1] Graduate school of Mechanical Engineering
[2] Department of Mechanical Engineering
Tokyo University of Science, Japan
[3] CMS Co. Ltd., Japan

Abstract

Recently, the equipment to separate and classify nano-size particles are required in various areas. The objective of the present study is a new solid-liquid separator, which enables us to separate and classify nano-size particles, to cut down the water content ratio of disposed particles and to accomplish extremely high collection efficiency. In this study, a numerical method is developed to simulate gas-liquid-solid three-phase flow, based on the moving particle semi-implicit (MPS) approach to clarify the flow field inside the separator and mechanism of particle separation. With using our method, some interactions of three phases that are difficult to be duplicated with the traditional grid methods are reproduced.

Keywords: flow modeling, three-phase flow, particle method, particle separator, centrifugal force, nano-scale particle.

1 Introduction

Nano-particle is expected to be very useful and promising as an advanced material in a great number of industries such as automobile, aeronautics, chemistry, pharmacy, food, military and so on. However, the production and collection of nano-particles are very difficult and cost consuming with current technologies. For example, the conventional particle separator, which is a so-called cyclone, can separate only few-micron-size particles from liquid (Stairmand (1985), Krishna et al.(2010)), and thus it cannot be applied to nano-particles separation. Therefore, we have to develop an innovative particle separator, and especially we need a specially-designed nano-particle separator. Conventionally, high performance separators adopt centrifugal force generated from a highly swirling flow or a rotating chamber, to separate particles from liquid. The flow is essentially of liquid-particle two-phase, highly swirling and turbulent. Moreover, the flow often has a liquid free surface in the core and air bubbles which are generated during separation process. Since these complex

flow natures prevent us from measuring and observing the flow and particle behaviors, the separation phenomena of particles from liquid have not been clarified yet. Hence, a numerical simulation is expected to be a useful analytical tool. However, the numerical procedure itself has not been established due to the difficulties in modeling and computing the multi-phase and multi-physics flow characteristics. Therefore, we need urgently and strongly to focus on the development of a new simulation technique that can sufficiently predict the complicated physics in a nano-particle separation process.

In the present study, taking into account the above backgrounds, we try to construct a new numerical modeling to reproduce the three-phase (i.e. liquid-particle-bubble) flow in a nano-particle separator. A specially-designed rotating-type particle separator is adopted as our computational target. It consists of coaxial rotating circular pipes. Particle-laden liquid is ingested from the top of the inner pipe. Since centrifugal force acting on particles in the liquid pushes the particles radially outward, the particles accumulate on the outer pipe surface, and the liquid forms a thick rotating film. It is noted that the centrifugal force can be about 3,000 times of gravitational force (i.e. 3,000G). In this separation process, air bubbles are often generated in the liquid film on the outer pipe surface. The mechanism of the bubble generation has not been clarified. It is known that the bubble formation degrades the separation performance. Finally, the accumulated particles are exhausted from the bottom of the outer pipe by the screw propeller mounted on the inner pipe. Figure 1 shows the schematic view of this separator. For this three-phase flow, a particle method is employed to model the motions of liquid, particle and air bubble by those of virtual particles. We use a MPS method as the base numerical procedure because of the simplicity and relatively good predictability for liquid flow and free surface. In our modeling, different particles with different diameters and densities are assigned to particles representing liquid, particle and bubble. In the present study, as the first step of this research, we focus on the bubble formation region. Investigating the numerical results, it is confirmed that the bubble generation process is naturally and satisfactorily reproduced by the particle method proposed in the present study.

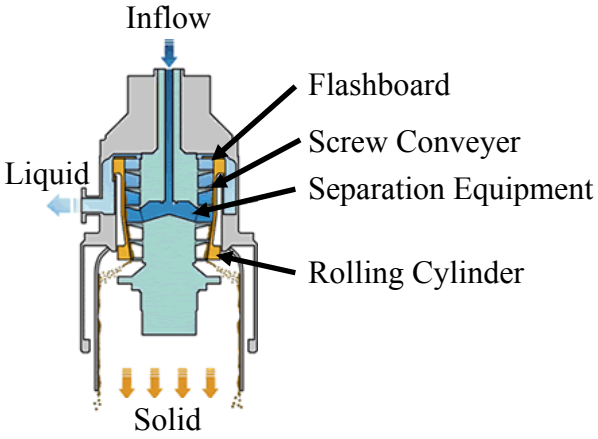

Figure 1: The schematic view of the nano-particle separator

2 Numerical Procedures

2.1 Single-phase flow

2.1.1 Governing equation

The governing equations of Navier-Stokes equation and incompressibility are expressed as follow:

$$\nabla \cdot \mathbf{u} = 0 \tag{1}$$

$$\frac{\mathrm{D}\mathbf{u}}{\mathrm{D}t} = -\frac{1}{\rho}\nabla P + \nu\nabla^2\mathbf{u} + \mathbf{F}\,. \tag{2}$$

In a MPS method, Navier-Stokes equation is divided into pressure part and other part as follows.

$$\left(\frac{\mathrm{D}\mathbf{u}}{\mathrm{D}t}\right)^{\mathrm{press}} = -\frac{1}{\rho}\nabla P \tag{3}$$

$$\left(\frac{\mathrm{D}\mathbf{u}}{\mathrm{D}t}\right)^{\mathrm{other}} = \nu\nabla^2\mathbf{u} + \mathbf{F} \tag{4}$$

Time derivation of Equation(1) can be expressed by

$$\nabla \cdot \left(\frac{\mathrm{D}\mathbf{u}}{\mathrm{D}t}\right)^{\mathrm{press}} + \nabla \cdot \left(\frac{\mathrm{D}\mathbf{u}}{\mathrm{D}t}\right)^{\mathrm{other}} = 0\,. \tag{5}$$

Then the continuity equation is given by

$$\frac{\mathrm{D}\rho}{\mathrm{D}t} + \rho\nabla \cdot \mathbf{u} = 0\,. \tag{6}$$

From Equations(3) to (6),

$$-\nabla \cdot \frac{1}{\rho}\nabla P = \frac{1}{\rho^0}\left(\frac{D^2\rho}{Dt^2}\right) \tag{7}$$

is obtained. In Equation(7) the relation that density ρ is equal to constant density ρ^0 with incompressible fluid is taken into account.

2.1.2 Discretization

The governing equations of Navier-Stokes and continuity equations involve gradient

and Laplacian. In a MPS method, gradient and Laplacian models are prepared to solve the governing equations. The models can be given as follows:

$$\nabla\phi = \frac{d}{n^0}\sum_j \frac{\phi_j - \phi_i}{\left|\mathbf{r}_{ij}\right|^2}\mathbf{r}_{ij} w_{ij} \tag{8}$$

$$\nabla^2\phi = \frac{2d}{\lambda n^0}\sum_j \left(\phi_j - \phi_i\right) w_{ij} \tag{9}$$

where ϕ is physical quantity, d is number of dimension, $\mathbf{r}_{ij}$ is interparticle distance $\mathbf{r}_{ij}=\mathbf{x}_j-\mathbf{x}_i$ and subscripts i, j are the numbers for particle indentification. n_i is particle number density that is calculated by

$$n_i = \sum_j w_{ij} \tag{10}$$

and the particle number density calculated with initial particle position is n^0, and initial particle number density λ is calculated with regular particle position of initial state as follow:

$$\lambda = \frac{\sum_j \left|\mathbf{r}_{ij}\right|}{\sum_j w_{ij}}. \tag{11}$$

w_{ij} is a weighting function and weights the interaction according to the interparticle distance $\mathbf{r}_{ij}$. The weighting function w_{ij} is generally given by

$$w_{ij} = \begin{cases} \dfrac{r_e}{\mathbf{r}_{ij}} - 1 & \left|\mathbf{r}_{ij}\right| < r_e \\ 0 & \left|\mathbf{r}_{ij}\right| \geq r_e \end{cases} \tag{12}$$

where r_e is influence radius. The closer particles are, the more influences operate between the particles with this weighting function. And particles having interparticle distance larger than influence radius r_e do not interact with each other.

2.1.3 Calculation algorithm

Two-stage algorithm is employed in a MPS method and the time step is divided into two stages. In the first stage, all terms of Equation(2) except pressure term are calculated and the temporal velocities $\mathbf{u}^*$ and positions $\mathbf{x}^*$ of all particles are predicted. Then, the temporal values are corrected by pressure term, and the actual velocities $\mathbf{u}^{k+1}$ and positions $\mathbf{x}^{k+1}$ are calculated in the second stage.

First, the value of Equation(4) is calculated with using Equation(9) and the temporal values are expressed as follows:

$$\mathbf{u}^* = \mathbf{u}^k + \Delta t\left(\frac{\mathrm{D}\mathbf{u}}{\mathrm{D}t}\right)^{\text{other}} \tag{13}$$

$$\mathbf{x}^* = \mathbf{x}^k + \Delta t\mathbf{u}^* . \tag{14}$$

Then, the right-hand side of Equation(7) is

$$\frac{1}{\rho^0}\left(\frac{\mathrm{D}^2\rho}{\mathrm{D}t^2}\right) = \frac{1}{\Delta t^2}\frac{n_i^* - n^0}{n^0} \tag{15}$$

where n_i* is particle number density calculated from temporal values. Equation(15) is based on the concept that density is proportional to particle number density. Furthermore, by discretizing the left-hand side of Equation(7), pressure is calculated. At this time, pressure of the particles on the interface which satisfy

$$n_i < 0.8n^0 \tag{16}$$

is fixed to zero. And, if there are particles having negative pressure, pressures of the particles are corrected to zero.

Then, Equation(3) is obtained with using Equation(8) and the velocities $\mathbf{u}^{k+1}$ and positions $\mathbf{x}^{k+1}$ are calculated as follows:

$$\mathbf{u}^{k+1} = \mathbf{u}^* + \Delta t\left(\frac{\mathrm{D}\mathbf{u}}{\mathrm{D}t}\right)^{\text{press}} \tag{17}$$

$$\mathbf{x}^{k+1} = \mathbf{x}^* + \Delta t^2\left(\frac{\mathrm{D}\mathbf{u}}{\mathrm{D}t}\right)^{\text{press}} \tag{18}$$

2.2 Gas-liquid two-phase flow

In this study, liquid-gas two-phase flow simulation is performed by dividing the pressure calculation into two steps. This computational method is employed to prevent gas-phase particles from flying away by the continuous pressure gradient on the gas-liquid interface and gas, liquid-phase particles are calculated at the same time about the prediction of particle velocity and position with Equations(13) and (14).

In the first step, only liquid-phase particles are calculated ignoring the gas-phase particles. At this time, pressures of the liquid-phase particles on the gas-liquid interface are fixed to the pressure of neighbouring gas-phase particle. In this way, the influences of gas-phase are transfer to the neighbouring liquid-phase particles. In the second step, the liquid particles that are calculated in the first step are treated as wall particles, and the calculation for only gas-phase is carried out.

By separating the liquid-phase and gas-phase calculation, it is not necessary to treat gas-phase and liquid-phase particles that have large density difference at the same time and the instability of calculation derived from the large density difference that is the main problem for two-phase flow simulation with a MPS method is avoided.

2.3 Gas-liquid-solid three-phase flow

Three-phase flow is simulated by combining the two-phase flow simulation described above and trajectory calculation of solid particles. The particle trajectories are calculated with a Lagrangian approach. Particles are assumed to be spherical and irrotational. Gravity and hydrodynamic drag are considered as forces acting on the solid particles. The motion equation of a solid particle is given as

$$\frac{\mathrm{D}\mathbf{u}}{\mathrm{D}t} = \mathbf{F}_G + \mathbf{F}_D \tag{19}$$

where $\mathbf{F}_\mathrm{G}$ is gravity and $\mathbf{F}_\mathrm{D}$ is aerodynamic, hydrodynamic drag acting on solid particles from gas-phase and liquid phase. The drag is expressed as follow:

$$\mathbf{F}_D = \frac{3C_D\rho_f}{4\rho_s D_p}\left(\mathbf{u}_f - \mathbf{u}_p\right)\left|\mathbf{u}_f - \mathbf{u}_p\right| \tag{20}$$

$$\mathrm{Re}_p = \frac{D_p\left|\mathbf{u}_f - \mathbf{u}_p\right|}{\nu_f} \tag{21}$$

$$C_D = \begin{cases} \dfrac{24}{\mathrm{Re}_p}\left(1 + 0.15\mathrm{Re}_p^{0.687}\right) & (\mathrm{Re}_p < 1000) \\ 0.44 & (\mathrm{Re}_p \geq 1000) \end{cases} \tag{22}$$

where C_D is drag coefficient, D_p is particle diameter, Re_p is particle Reynolds number and subscripts *f* and *s* represent fluid(gas or liquid) and solid, respectively.

3 Computational Conditions

In this study, we conducted a numerical test for a dam break phenomenon with single-phase simulation, gas-liquid two-phase simulation and an air-bubble engulfments phenomenon with gas-liquid-solid three-phase simulation. The computational domains of the dam break and the air-bubble engulfments phenomena are shown in Figures 2(a) and (b), respectively. The computational conditions are listed in Table 1.

Particle spacing		0.12[m]
Gas-phase	Density	1.205[kg/m^3]
	Kinematic viscosity	15.12×10^{-6}[m^2/s]
Liquid-phase	Density	998.2[kg/m^3]
	Kinematic viscosity	1.004×10^{-6}[m^2/s]
Solid-phase	Density	2.2×10^{3}[kg/m^3]

Table 1: Computational conditions

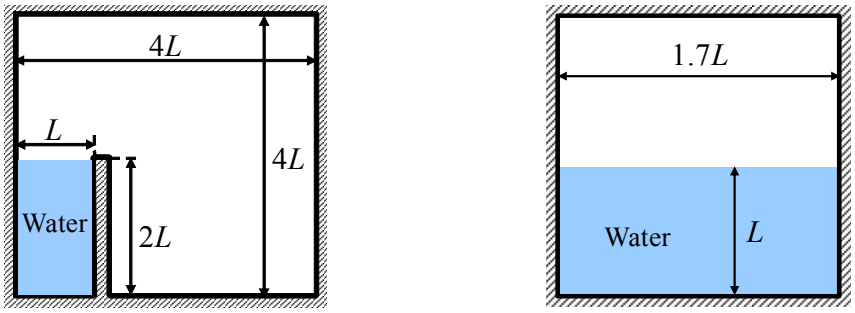

(a) Dam break phenomenon (b) Engulfments phenomenon

Figure 2: Computational domains of the dam break problem

In the dam break phenomenon, collapse of water column is observed when the dam is removed instantaneously as shown in Figure 3. Note that the width of the water column, L = 0.864[m] is employed, and the operating fluids are water as liquid-phase and air as gas-phase.

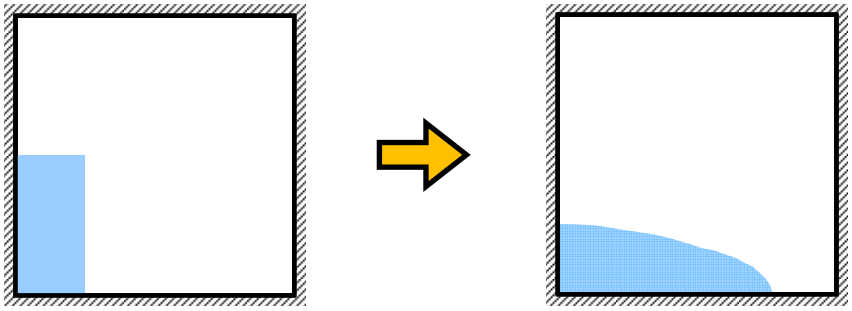

Figure 3: Schematic of dam break phenomenon

In the air-bubble engulfments phenomena, free-fallen solid particles from certain height impact on the gas-liquid interface and the air-bubbles are engulfed into the water as illustrated in Figure 4. This situation mimickes the phenomenon occurred in the advanced particle separator(see Figure1). The computational domain is exhibited in Figure 2(b) and the depth of the water L = 0.36[m] is employed. The operation materials are air as gas-phase, water as liquid-phase and diatom earth as solid-phase.

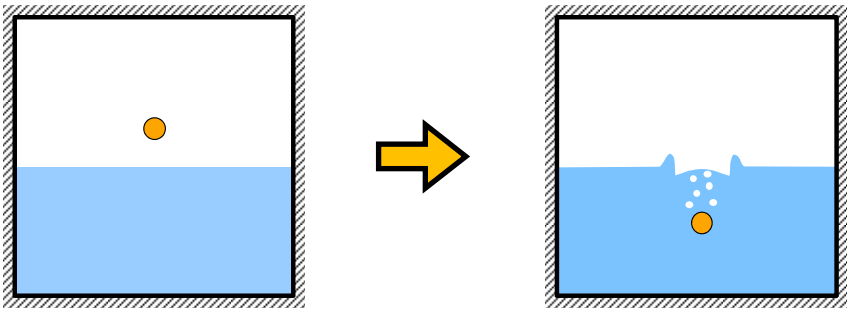

Figure 4: Schematic of air-bubble engulfments phenomenon

4 Results and Discussion

4.1 Liquid single-phase flow

In this section, we focus on the dam break phenomenon simulated with liquid single-phase simulation. Figure 2(a) exhibits the schematic of dam and the computational domain. And comparisons of computational and experimental result are shown in Figure 5. The left side figures are the experimental results measured by Koshizuka et al.(1995) and right side ones are the computational results with the present MPS method. Yellow dots in the figures represent liquid-phase particles.

As shown in Figure 5, the computational results show the same trend with the experimental results and we can say that the simulation reproduces the dam break phenomenon reasonably.

Then, the quantitative comparison is exhibited in Figure 6.In Figure 6, L is the initial width of water column, Z is the position of leading edge of interface, t is elapsed time and T is the time when the leading edge of interface arrives at the right side wall. It is found that the computational and experimental results indicate reasonable agreement from Figure 6 as well as Figure 5. In Figure 6, computational results using VOF method is also shown with computational results using the MPS method and the experimental results. VOF method is one of the typical interface tracking methods with grid system and often used for two-phase flow simulations. From the comparison between the MPS method and VOF method, we can see particle method has advantages over grid method for the two-phase flow simulation. It would be caused from the unphysical diffusion in the VOF method.

Though the single-phase flow simulation shows reasonable agreement with the experimental results, it is difficult to duplicate the air bubbles that are generated inside the liquid-phase. Additionally, the MPS method can not keep its reliability in the area where the particle number density is not sufficient. These problems are resolved by filling up the no-particle-areas with gas-phase particles. So we focus on the gas-liquid two-phase simulation in next section.

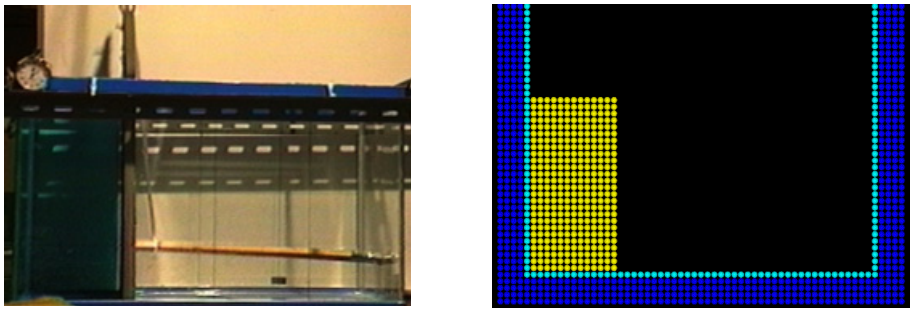

(a)t = 0.0[s]

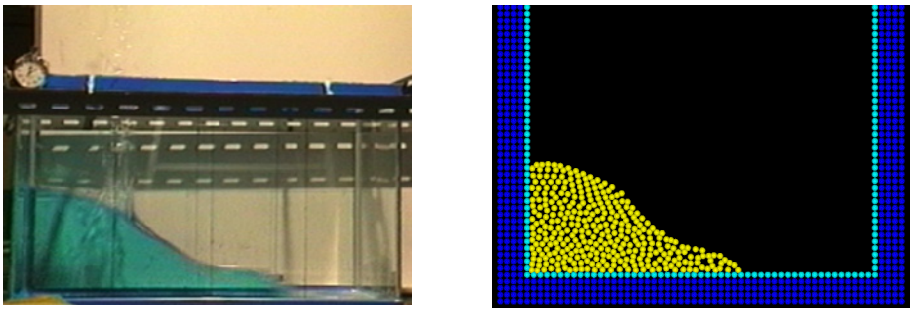

(b)t = 0.2[s]

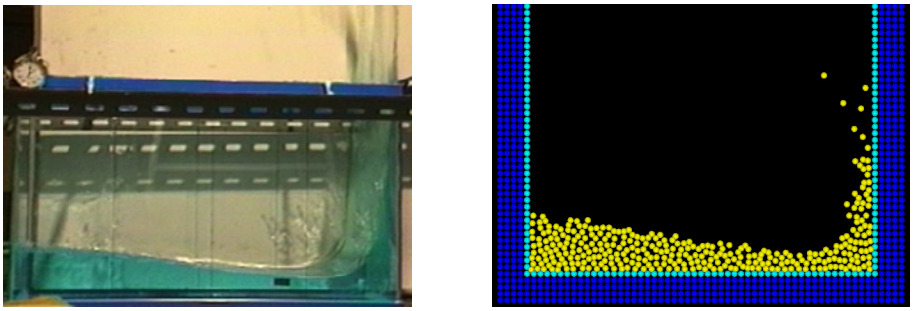

(c)t = 0.4[s]

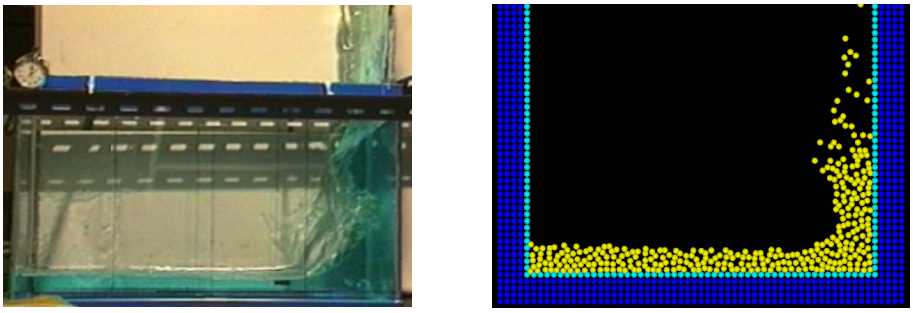

(d) t = 0.6[s]

Figure 5: Comparison of experimental result and single-phase simulation
(Left: Experiment, Koshizuka et al.(1995))

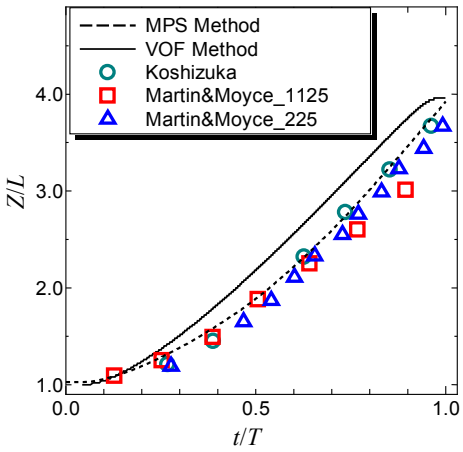

Figure 6: Validation of single-phase simulation

4.2 Gas-liquid two-phase flow

Gas-liquid two-phase simulation is discussed in this section. Gas-liquid two-phase simulation is conducted in the same conditions with the single-phase simulation. The comparison of single-phase simulation and two-phase simulation is shown in Figure 7. The right side figures are the results of two-phase simulation and the left side ones are the results of single-phase simulation. In this figure, yellow dots represent liquid-phase particles and red dots are gas-phase particles.

From Figure 7, single phase and two-phase simulations show the similar features. However, the two-phase simulation estimates the interface a little lower than the single-phase simulation. This is because the pressure of liquid-phase particles on the interface is fixed to zero in the single-phase simulation, while the liquid-phase particles on the interface have non-zero pressure to be equal to the neighbouring gas-phase particles. Additionally, gas-phase particles exist inside the liquid-phase, as clearly shown in Figure 7(d). It would appear that engulfment of air bubbles into the liquid is duplicated.

As shown in Figure 8, the interface behaviours of single-phase and two-phase simulation represent the similar trends. The difference between single-phase and two-phase simulations is derived from the maximum speed of interface. In the two-phase simulation, the maximum speed of interface is larger than that of the single-phase one. In the two-phase simulation, there are gas-phase particles over the liquid-phase particles column and the liquid-phase particles are accelerated more rapidly than the ones in the single-phase simulation at the earlier stage of dam breaking. In the same way, there are gas-phase particles between the interface and the right side wall, just before the liquid-phase particles reach the right side wall in the two-phase simulation. Because of these gas-phase particles, high pressure area is formed between the interface and the right side wall and liquid-phase particles decelerated more rapidly in the two-phase simulation than in the single-phase simulation.

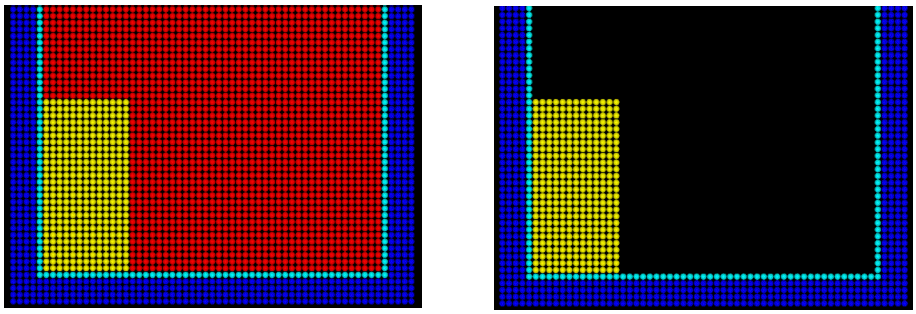

(a)t = 0.0[s]

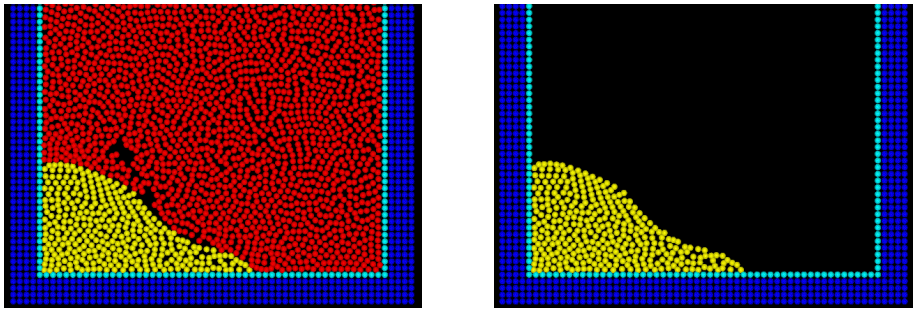

(b) t = 0.2[s]

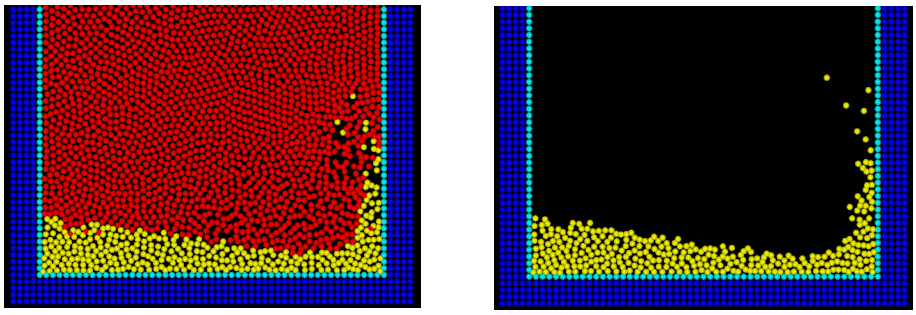

(c)t =0.4[s]

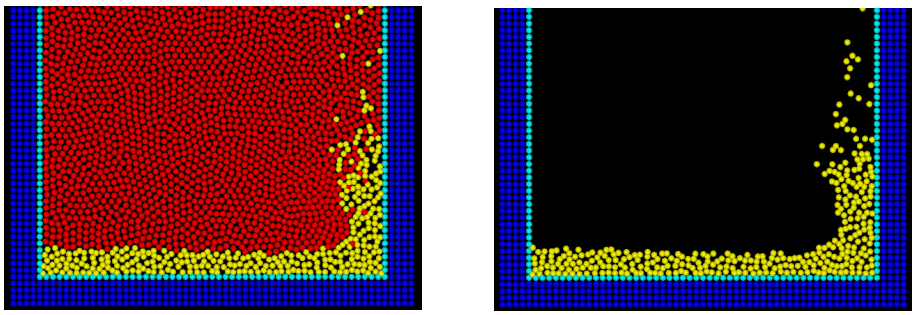

(d) t = 0.6[s]

Figure 7: Comparison of single-phase and two-phase simulation
(Left: two-phase, Right: Single-phase)

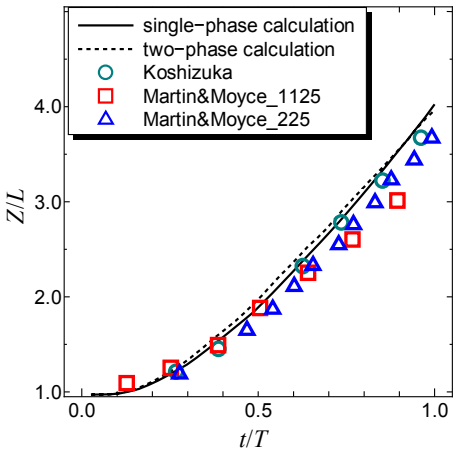

Figure 8: Validation of two-phase simulation

4.3 Gas-liquid-solid three-phase flow

In this section, the air-bubble engulfments phenomenon simulated with gas-liquid-solid three-phase simulation is discussed. The computational results are shown in Figure 9. Yellow, red, blue dots represent liquid-phase, gas-phase and solid particles, respectively.

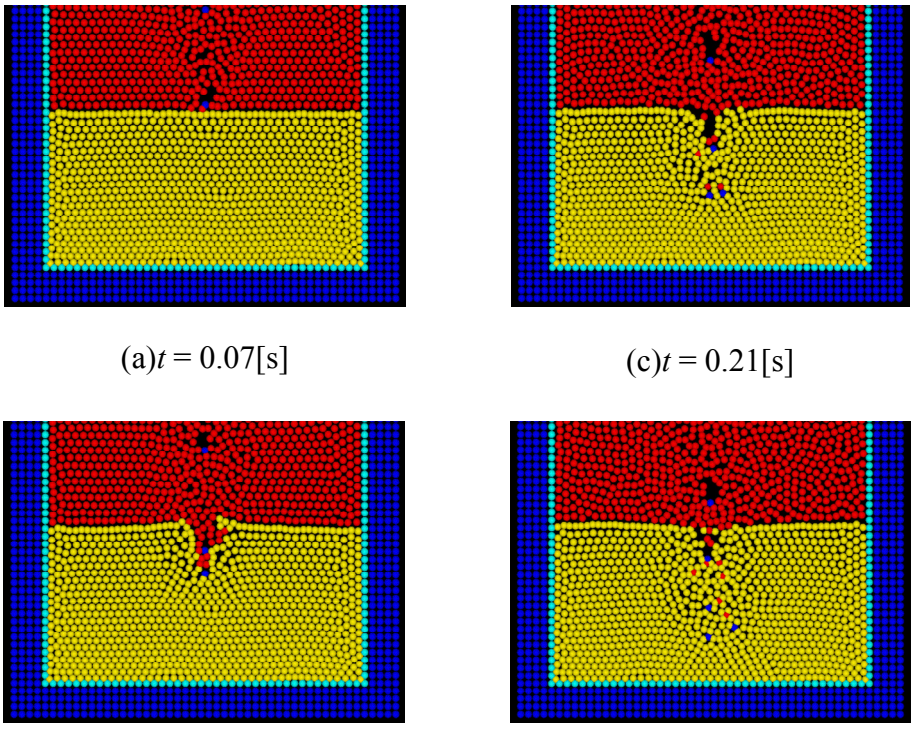

(a)t = 0.07[s]

(c)t = 0.21[s]

(b)t = 0.14[s]

(d)t = 0.28[s]

Figure 9: Engulfments of the air bubbles(red) into the water(yellow)

In Figure 9, the enguflments of air bubbles are apparently observed. Also, the velocity changes of solid particles in gas and liquid-phase is reproduced. The solid particles free-fall in gas-phase, then reduce their velocities rapidly with impacting to the gas and liquid-phase interface and sink by the density difference of solid and liquid in the liquid-phase. Furtermore, the interface is deformed by the impacts of solid particles. The interface bursts at the moment of solid particle impact, then the gas-phase particles go into the void space of liquid-phase particles. In this way, air bubbles are engulfed into the liquid-phase. These phenomena are difficult to be duplicated with use of the traditional grid methods, and thus it is confirmed that our MPS method has the ability to duplicate the interferences of gas, liquid and solid phases. However, the responsivities of the light particles to the faster heavy particles are not completely predicted and some no-particle spaces can be found behind the solid particles in Figure 9. Additionally, the second problem that should be improved is the need to match the gas and liquid-phase particles sizes with solid particles.

5 Conclusion

In this study, we developed a numerical method to simulate gas-liquid-solid three-phase flow, based of the MPS approach. We conducted some numerical tests with liquid single-phase, gas-liquid two-phase, gas-liquid-solid three-phase simulations. Those are dam break phenomenon with liquid single-phase and gas-liquid two-phase simulations and air-bubble engulfment phenomenon with gas-liquid-solid three-phase simulation. In the dam break simulations, code validations are conducted and both of the two computational results indicated reasonable agreement with the experimental results. In the air-bubble engulfment simulation, our numerical method duplicated some interactions of gas, liquid and solid phases that are difficult to be duplicated with the traditional grid methods. In our future works, we are planning to improve the present numerical method, and apply it to the actual particle separator, in order to clarify the three-phase flow characteristics.

References

[1] S. Koshizuka, H. Tamako, Y. Oka," A particle method for incompressible viscous flow with fluid fragmentation", Computational Fluid Dynamics Journal, 4, 29-46, 1995

[2] V. Krishna, R. Sropriya, V. Kumar, S. Chakraborty, B.C. Meikap, "Identification and Prediction of Air Core Diameter in a Hydro Cyclone by a Novel Online Sensor Based on Digital Signal Processing Technique", Chemical Engineering and Processing: Process Intensification, 49(2), 165-176, 2010

[3] J.C. Martin, W.J. Moyce, "An experimental study of the collapse of liquid columns on a rigid horizontal plane", Philos. Trans. Roy. Soc. London, Ser. A 244, 312-324, 1952

[4] C.J. Stairmand, "The Design and Performance of Cyclone Separators", Tans. Inst. Chemical Engineering, 29, 356-383, 1985